An experimental and predictive study of the tumbling generating characteristics of four-value cylinder heads under steady flow conditions

Seeley, W.A. , Baker, P., Girgis, N.S. and Benjamin, S.F.

S209

A Seminar organised by the Automobile Division
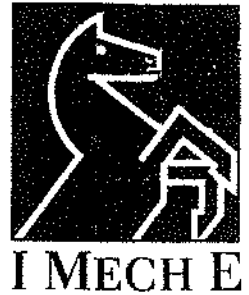
I MECH E

First IMechE Seminar on:

THE VALIDATION OF COMPUTATIONAL TECHNIQUES IN VEHICLE DESIGN -

Stage One:

COMPUTATIONAL FLUID DYNAMICS (CFD)

Date: Monday 18 April 1994

Venue: Institution of Mechanical Engineers,

1 Birdcage Walk, London, SW1H 9JJ

AN EXPERIMENTAL AND PREDICTIVE STUDY OF THE TUMBLE GENERATING CHARACTERISTICS OF FOUR-VALVE CYLINDER HEADS UNDER STEADY FLOW CONDITIONS

W A Seeley, P Baker, N S Girgis and S F Benjamin
Coventry University

ABSTRACT

An experimental and predictive study has been conducted on the tumbling generating characteristics of a four-valve cylinder head under steady flow conditions. This was conducted on a idealised cylinder head with a disc combustion chamber and two straight axisymmetric intake ports equipped with shrouded valves.

The tumbling generating characteristics of each intake configuration were evaluated using a steady flow rig which converted tumble into swirl. Experimental measurements of the swirl and axial velocity distributions for various valve lifts were obtained using laser Doppler anemometry. Theoretical predictions were performed using a commercial computational fluid dynamics (CFD) code. Comparisons have been made between the experimental results and theoretical predictions.

1.0 INTRODUCTION

Due to more stringent European emissions standards there has been an increasing need to develop and design combustion chambers that reduce emissions and give better fuel economy. Studies have recently shown [1] that a swirling motion perpendicular to the cylinder axis (barrel swirl) can be used to enhance pre-ignition turbulence levels and hence increase the flame speed. This increase can allow engines to run with ever increasing charge dilution (lean burn) and enhance the engine's tolerance level to exhaust gas recirculation (EGR). The increase in turbulence level has been shown to be highly dependent on the inlet port geometry and chamber shape. This has the desired effect of reducing emissions of CO and NO_X with improved fuel economy. However, to optimise the barrel swirl combustion system it is necessary to match the swirl level to the chamber shape to obtain the correct flow field at ignition.

The three main tools available to the design engineer are experimental techniques, phenomenological models and CFD predictions. Experimental techniques such as laser Doppler (LDA) and hot wire anemometry (HWA) can be very expensive and time consuming due to the necessity of having to manufacture and test each design modification. Although these experimental techniques are well established and can give accurate pictures of the flow field within production engines [2,3], they are limited to accessibility in the engine. Phenomenological models have been developed to examine barrel swirl flows[4] but are restricted to simple engine geometries, and require specification of the form of the flow field. In principle CFD allows predictions of the entire flow domain with rapid assessment of minor design modifications. Hence the development cost of such engines will be greatly reduced if CFD could confidently be used to predict swirling motion within the cylinder. Specific CFD codes have been written to predict swirling flows within simple engine geometries [5], but to date, commercial CFD codes have had limited application to this type of problem.

A research programme is underway to examine both experimentally and theoretically the flow field in barrel swirl chambers. The programme involves both steady state flow rig studies, and motored engine investigations. The objectives of the steady flow studies are :

   a) To examine the effect of port geometry on generating swirl.
   b) To assess the performance of a commercially available CFD code for steady flow simulations.
   c) To provide boundary conditions for the motored studies.

This paper describes the results from the steady state flow studies. A description of the steady state flow rig, and the HWA and LDA procedures used to obtain the boundary conditions and validation data is provided. The approach to the CFD simulations is outlined by a description of the

computational grid, the boundary conditions used and the solution procedure adopted. The results presented are a detailed analysis of the velocity profiles for the 10mm valve lift. Simulations of other valve lifts are underway.

2.0 EXPERIMENTAL SYSTEM

The steady flow tests were undertaken on the flow rig shown schematically in Figure (1) with air drawn through the cylinder head by a centrifugal fan. A Ricardo viscous flow air meter was used to measure the flowrate through the system. The upstream stagnation pressure was measured at the inlet plenum chamber. The pressure difference between the upstream stagnation and downstream static pressure was measured by a single limb water manometer, and controlled by a throttle attached to the outlet plenum chamber.

The test section consisted of a disc head with two straight axisymmetric ports equipped with shrouded valves to generate a tumbling motion within the cylinder. The 84 mm diameter cylinder has been fitted with a circular adapter, which converts the in-cylinder tumbling motion into swirl whilst allowing free passage of the air from the cylinder. This tumble tube adapter has the same bore as the cylinder. The LDA measurement plane is located at 2 x 84 and 3 x 84 mm along the adapter. The adapter has been extended a further 3.5 x 84 mm to ensure full development of the swirling motion. The cylinder provides a physical boundary close to the valve curtain area to prevent the air exiting straight out of the tumble tube adapter. A piston crown is simulated by a flat plate placed at the bottom of the cylinder; this is crucial for the development of the tumbling motion.

2.1 EXPERIMENTAL TECHNIQUES

2.1.1 LASER DOPPLER ANEMOMETRY

A single component fibre-optic LDA system was used to measure the axial and swirl velocity profiles at the two measuring planes in the tumble tube adapter. Figure (2) shows the basic arrangement of the system, which consists of,

      (a)   A 3 Watt Argon-Ion laser,
      (b)   An optical unit incorporating miniature optics for beam splitting and Bragg cells for frequency shifting,
      (c) A fibre-optically linked transmission and reception probe.

Table (1) details the specifications of the LDA system. The system was operated in back scatter where the light was scattered by particles of Titanium Dioxide (TiO_2). The TiO_2 seeding was supplied from an air jet atomiser into the inlet plenum chamber, which gave rise to an average particle diameter of 0.3 to 0.5 microns. The output from the photo multiplier tube was processed by a burst correlator (TSI IFA750) interfaced to a rotating machinery resolver (TSI 1989) and a microcomputer.

The mean velocity and turbulent velocity fluctuations were calculated from ensemble averaged estimates using 1000 data points. There are numerous sources of experimental error associated with the LDA technique [6], the main sources being velocity gradient broadening, velocity biasing, and uncertainties from using a finite sample size when performing averages. The flow statistics for mean velocity and turbulent velocity fluctuations were observed and no unusual deviations from a normal distribution were detected. The sample size was increased and no significant changes in the results were observed. From repeatability studies taken with the swirl velocity profiles, the accuracy of this technique is estimated to be within 4%.

Wavelength	514 nm
Beam separation	8 mm
Focal length	50 mm
Beam intersection at half angle	4.57°
Measuring volume width	0.122 mm
Measuring volume length	1.52 mm
Calibration constant	3.23 ms^{-1}/MHz
Frequency shift	10 MHz

Table 1 Specifications of LDA system

2.1.2 HOT WIRE ANEMOMETRY

The inlet valve curtain velocity profiles used for the CFD boundary conditions were taken using a DISA type 55P11 single wire probe connected to a DISA 55M10 CTA standard bridge and 55M01 main unit. The output signal from the bridge was fed into a DC voltmeter to obtain mean voltages.

The velocity profiles were obtained as axial, radial and tangential velocity components in a co-ordinate system relative to the valve periphery. To obtain the velocity components, a method similar to Catania [7] was used. Measurements were taken every 15° around the valve circumference, and at 2mm intervals axially over the valve lift area.

To allow velocity measurements over a wide range of velocities, a second order response equation [8] was used in the calibration of the hot wire probe. To simplify the calibration curve it was assumed that the pitch factor was unity, and the yaw factor remained constant and was calculated from measurements taken during calibration with the hot wire parallel to the flow direction. The accuracy of this technique was assessed by placing the hot wire in various positions relative to a known flow field, and comparing the measured and actual velocities. It was found that the velocity magnitude could be measured to an accuracy of within 5%, whilst the direction could be measured to within 5°.

2.2 CFD SIMULATIONS

The simulations were conducted on a Silicon Graphics Indigo R4000 using the commercial CFD code STAR-CD.

2.2.1 COMPUTATIONAL GRID

The steady flow rig was modelled as close to reality as possible, (see figure 3). The grid was produced using Prostar, the pre/post processor STAR-CD. It was built up from a series of splines to outline the overall geometry. From these splines meshed blocks were created to suit the geometry. Blocks are volumes defined by specifying the eight corners of the volume and then subdividing each edge to create a set of computational grid cells. Blocks were used to aid the modelling of the complex geometry and to facilitate mesh refinement. A base block arrangement was developed, using the head face geometry including the positioning of the valves. This base grid was then

projected throughout the computational domain to create the entire mesh. Varying the thickness of the head face blocks allowed for different valve lifts to be modelled, with simple adjustment to the remaining geometry. The position of the valve curtain area was created by removing the two inlet port blocks from the head face and then applying inlet conditions on the correct cell faces.

2.2.2 BOUNDARY CONDITIONS

The inlet conditions were applied based on the HWA measurements taken around the valve curtain. They were applied at 15° increments around the valve and at 2mm intervals axially from the head face over the entire valve lift. The inlets specified the three components of velocity in the radial, tangential and axial directions U, V and W respectively, density ρ; kinetic energy k and its dissipation rate ε and temperature T. This allowed for the correct inlet mass flow rate to be obtained. A standard outlet was applied across the end of the tumble tube with all the flow passing across this boundary. The wall boundary condition applied was that of the adiabatic no-slip kind, using wall functions in the near wall region.

Other simulations were conducted as follows. Initially the inlet plenum chamber was modelled by creating two large bellmouths placed at the beginning of the inlet ports. Pressure boundaries were applied across the faces of the bellmouths and the outlet face of the tumble tube. This was conducted to avoid the need for taking extensive experimental data around the valve curtain area. However modelling the inlet plenum gave rise to incorrect mass flow rate predictions. Simulations were also carried out modelling the outlet plenum. This was to allow the flow to develop along the entire length of the tumble tube and to facilitate any reverse flow. It was found that modelling the outlet plenum gave no noticeable difference to the results for the cases reported here. Therefore all simulations were carried out without modelling either inlet or outlet plenums.

2.2.3 SOLUTION PROCEDURE

STAR-CD employs the finite volume method for solving the Reynolds averaged Navier Stokes equations. The flow was assumed compressible and was solved using the Ideal Gas Law. The SIMPLE solution algorithm was used [9]. The solution procedure was split into three phases. Initial calculations were conducted using the upwind differencing (UD) scheme and the standard k-ε turbulence model. The second phase employed a self-filtered central differencing scheme (SFCD) to help reduce numerical diffusion in the tumble tube region. This scheme is effectively central differencing with a localised blend of central differencing with upwind differencing to reduce numerical diffusion without dispersion. The final phase was to switch the turbulence model over to the RNG variation of the k-ε model. During the final phase there was also the need to adjust the under relaxation factors for the velocity components to aid convergence. This procedure was conducted on two sizes of grid. A coarse grid of 70000 cells and a finer grid of 200000 cells were used to try and obtain a grid independent solution. All solution procedure details can be found in the STAR-CD user guide [10].

3.0 RESULTS AND DISCUSSION

The results presented show a detailed analysis of the axial and swirl velocity profiles in the tumble tube adapter for the 10mm valve lift. During the presentation of these results, reference is made to the section A-A and B-B of the measuring planes. Section A-A is defined as running perpendicular to the head face, whilst B-B is parallel to the head face. The measuring planes can be seen in figure 4. Swirl velocity is defined as the mean instantaneous velocity parallel to the measuring plane. Axial velocity is the mean instantaneous velocity perpendicular to the measuring plane.

3.1 COARSE GRID SIMULATIONS

3.1.1 STANDARD k-ε AND UPWIND DIFFERENCING

Axial and swirl velocity profiles were taken at the three bore measuring plane in the tumble tube. A comparison of the experimental and CFD upwind differencing axial velocity profiles can be seen in figures 5a & 5b. It can be seen from these profiles that the minimum velocity tends towards zero, and is off centre from the axis of the tumble tube. The velocity magnitudes near the wall differ due to the corkscrewing effect of the swirling flow down the tumble tube. Poor correlation is achieved. In particular the CFD simulations incorrectly predict the minimum velocity point in both position and magnitude. The velocity magnitude in the higher velocity region of the flow reveals a closer comparison than in the lower velocity flow region.

From the experimentally determined swirl velocity profiles shown in figures 6a & 6b, it can be seen that the zero velocity point lies off centre of the tumble tube. The magnitude of the velocity on both sides of the tube remain approximately constant towards the edge, with the central region exhibiting solid body rotation. The swirl velocity profiles obtained from the CFD simulations give a straighter profile approaching solid body rotation. Comparison of the swirl profiles reveals that the CFD simulation incorrectly positions the swirl centre, and under predicts the swirl magnitude by approximately 50%. For this reason a second swirl profile comparison was made by taking measurements at the two bore measuring plane. Figures 7a & 7b show the vertical and horizontal swirl velocity profile comparison at the different measuring planes. It can be seen that the experimentally determined swirl magnitude does not decay considerably along the tube, hence swirl momentum is shown to be conserved. The main difference between the two and three bore swirl profiles is the movement of the swirl centre to the opposite side of the tube. This indicates that the swirl centre precesses slightly along the tumble tube. Conversely the CFD predictions show a dramatic decrease in the swirl velocity magnitude as the measuring point is moved from one bore to three bore. The solid body type rotation still persists throughout the three measuring points. There are several possible reasons for the CFD predicting the swirl decaying along the tube :

   a) Numerical diffusion due to the use of a first order differencing scheme to solve the finite volume equations.
   b) Incorrect turbulence modelling.
   c) The grid being too coarse.

3.1.2 SFCD

In an attempt to reduce numerical diffusion and keep computational time to a minimum, the SFCD higher order differencing scheme was used and the results are shown in figures 5 and 6. A comparison of the axial flow profiles (figure 5) shows that the SFCD has a similar velocity gradient to the UD in the higher velocity region, although the velocity at the wall is more in line with the experimental data. The minimum velocity point is again overpredicted. In the lower velocity region the SFCD and UD show similar velocity gradients, although the experimental velocity gradient is marginally steeper. These trends can be seen in both the vertical and horizontal measuring planes in figures 5a & 5b.

The swirl profiles exhibit an improvement of over 20% in velocity magnitude in the near wall regions. The general form of the swirl profiles with the positioning of the swirl centre and the solid body rotation type flow remaining relatively unchanged.

3.1.3 RNG + SFCD

Figures 5 and 6 show the effect of using the RNG modelling option with the SFCD scheme. The axial velocity profiles show a much better trend with the minimum velocity magnitude being more comparable with the experimental results. The magnitude of these predictions in the near wall region are similar to the SFCD. Predictions are also improved in the lower velocity regions across the tube.

The swirl velocity profiles show little or no difference to that found using the SFCD scheme with the standard k-ε turbulence model.

3.2 GRID REFINEMENT

The computational grid was increased from 70000 cells to 200000 cells. Grid refinement was undertaken in the axial direction down the tumble tube. This has the effect of reducing the cell aspect ratios in the flow direction from approximately 5 to less than 3.7.

The axial velocity profiles in section A-A, show a similar form to the other CFD simulations. In the lower velocity regions, the correlations are slightly improved. The minimum velocity value remains the same as for the previous simulation. For the section B-B the profile and magnitudes remain unchanged from the RNG + SFCD simulation over the full diameter of the tumble tube.

Little or no change was found in the swirl velocity profiles in either section A-A or B-B. This could be due to the relatively coarse grid resolution in the swirl plane. Further simulations are underway to analyse the effect of grid refinement in the swirl direction.

3.3 OTHER VALVE LIFTS

The experimentally determined data for various valve lifts can be seen in figures 8a & 8b. These results are taken for the axial and swirl velocity profiles at the three bore measuring plane along section A-A. The range of valve lifts covered is 2 mm to 10 mm in 2 mm intervals. For all tests, the pressure difference across the test section remained constant at 200 mm/H_2O.

The axial results show a general decrease in velocity magnitude as valve lift is decreased. The velocity profile trends for valve lifts less than 6 mm are similar, with the minimum velocity magnitude located in the centre of the tube. For the higher valve lifts, the minimum velocity is off centre. As the valve lift decreases, it is interesting to note that generally a higher back flow towards the cylinder occurs at the centre of the tube.

The swirl velocity profiles show a similar form for all valve lifts. The magnitudes of these profiles for valve lifts less than 8 mm decrease uniformly with valve lift. The 8 mm and 10 mm valve lift profiles are almost identical in magnitude due to port restriction. In general the swirl centre does not remain in one position, but moves around the central core of the tumble tube. This could be due to differences in the inlet flow. It was observed that the valve curtain velocity profiles at the higher lifts produce a narrower jet like structure, whereas the lower lifts tend towards a radially dispersed flow.

4.0 CONCLUSIONS

Comparisons of the axial and swirl velocity profiles in the tumble tube adapter of a steady state flow rig have been conducted between experimental data and CFD simulations. The following conclusions have been derived from this study :

a) CFD predictions of the axial velocity profiles within a swirling flow were obtained to a fair degree of accuracy.

b) The swirl velocity correlations were quite poor in both magnitude and form. Whether this is due to inadequacies in the grid refinement / numerical techniques or to the application of the k-ε model for swirling flows remains to be seen as part of future investigations.

c) The general form of the flow can be characterised as a corkscrewing effect travelling along the tumble tube, with the screw centre precessing around the axis of the tube.

ACKNOWLEDGEMENTS

REFERENCES

1. Benjamin, S.F., The development of the GTL 'Barrel Swirl' combustion system with application to Four-Valve spark ignition Engines, *Proc. Inst. Mech. Engrs*, Combustion in Engines - Technology and Applications, IMechE Conference, paper No. C323/049, p203, 1988.
2. Newman, A.W., Girgis, N.S. and Whiston, P.J., Laser Doppler Anemometer measurements in a four-valve pent roof combustion chamber, *Proc. Inst. Mech. Engrs*, paper No. C465/035, p283, 1993.
3. Witze, P.O., A critical comparison of Hot Wire Anemometry and Laser Doppler Velocimetry for I.C. engine applications, SAE 800132, 1980
4. Benjamin, S.F., Prediction of barrel swirl and turbulence in reciprocating engines using a phenomenological, IMechE Conference on Experimental and Predictive Methods in Engine Rsearch and Development, 17-18 Nov 1993 NEC, Birmingham paper L20/C465-013, p 87-101
5. Gosman, A. D., Tsui, Y. Y. and Vafidis, C. Flow in a model engine with a shrouded valve-a combined experimental and computational study. SAE 850498, 1985.
6. Edwards, R.V., editor, Report of the special panel on statistical particle bias problems in laser anemometry, *Presented at the Winter Annual Meeting of the American Society of Mechanical Engineers*, 1985
7. Catania, A.E., 3-D swirling flows in an open chamber automotive diesel engine with different induction systems.
8. Siddall, R.G. and Davies, T.W., An improved response equation for Hot-Wire Anemometry, *Int. J Heat Mass Transfer*, Vol. 15, p 367, 1972.
9. Patankar, S.V. and Spalding, D.B., A calculation procedure for heat, mass and momentum in three-dimensional parabolic flows, *Int. J Heat Mass Transfer*, vol. 15, 1972.
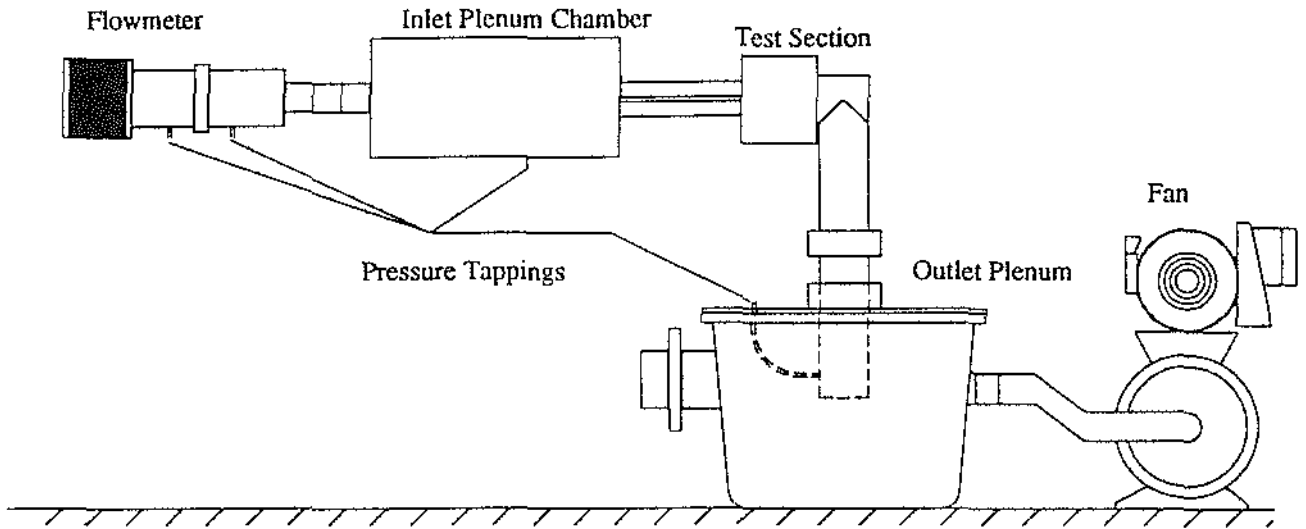10. STAR-CD Version 2.2 Manuals, Computational Dynamics Limited, 1993.
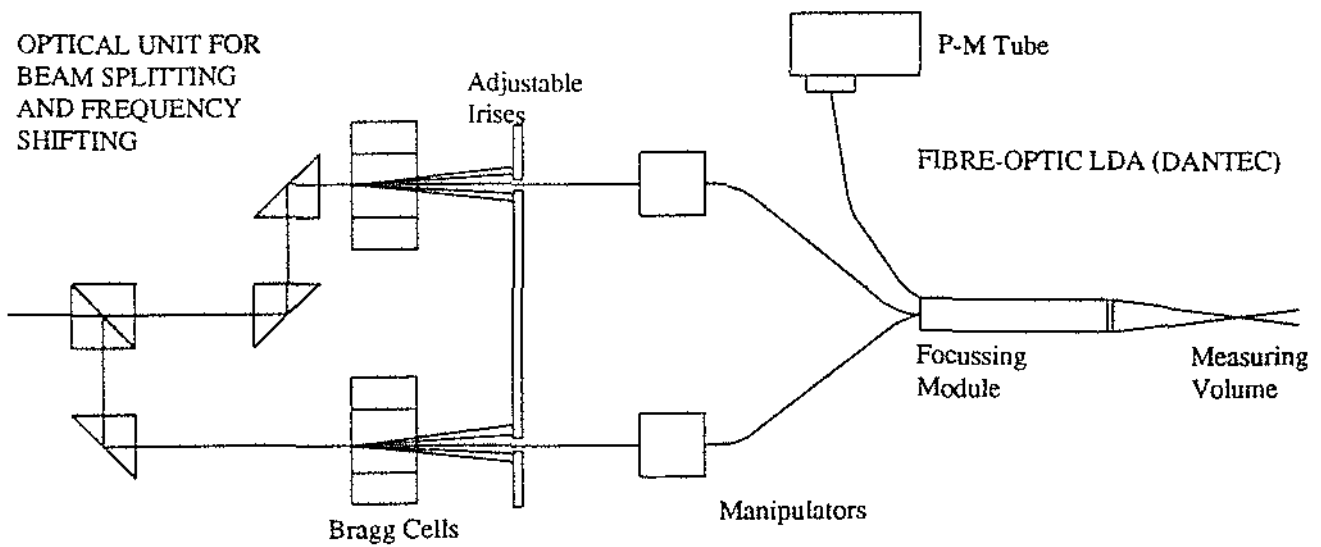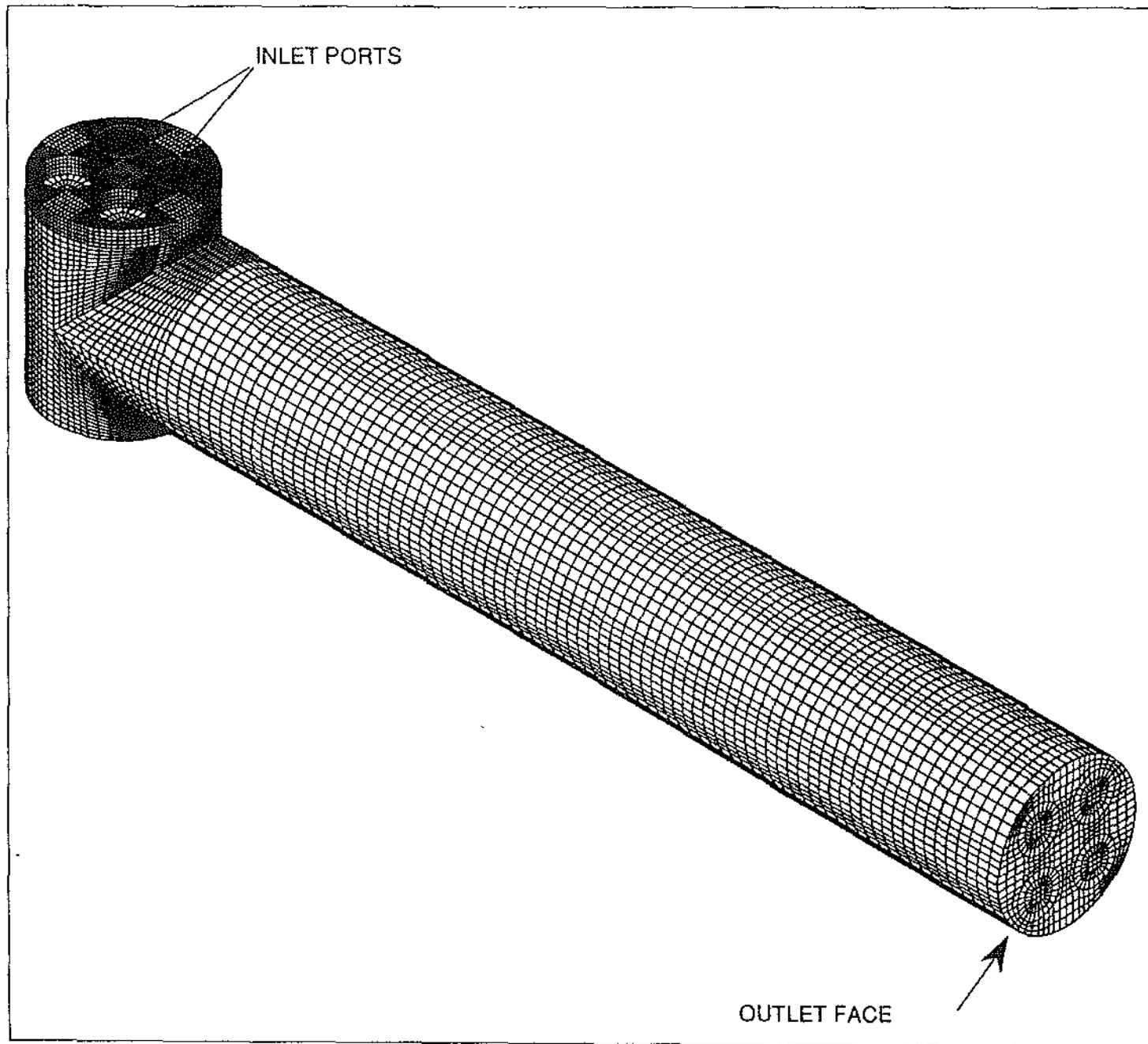
Figure 1 - Schematic of Steady State Flow Rig

Figure 2 - Optical Arrangement of the LDA System

INLET PORTS

OUTLET FACE

STAR

PROSTAR 2.2

07-Apr-94
VIEW
    1.000
    1.000
    1.000
ANGLE
    0.000
DISTANCE
    0.247
CENTER
    -0.011
    0.267
    -0.055
EHIDDEN PLOT
BOUNDARIES

Z

X   Y

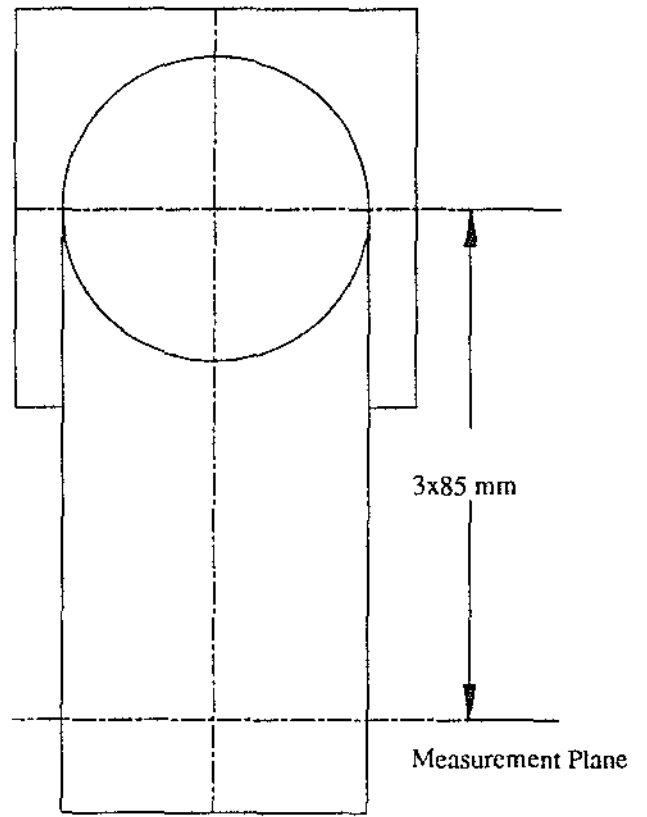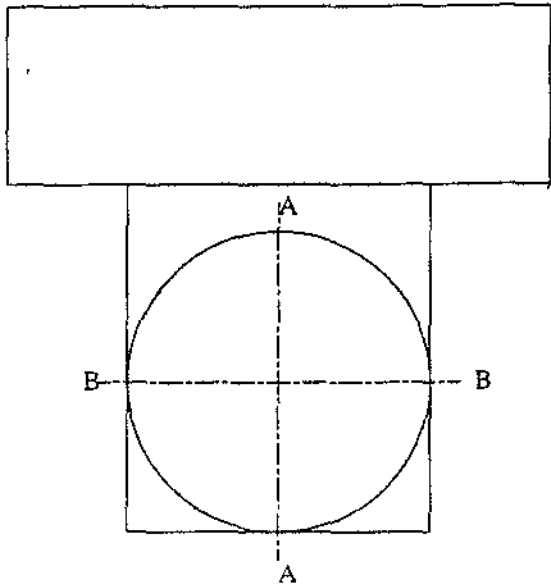Figure 3 - Computational Grid of the Steady StateFlow Rig.
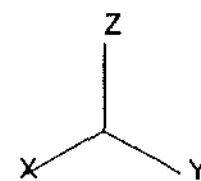
Figure 4 - Measurement Plane Location
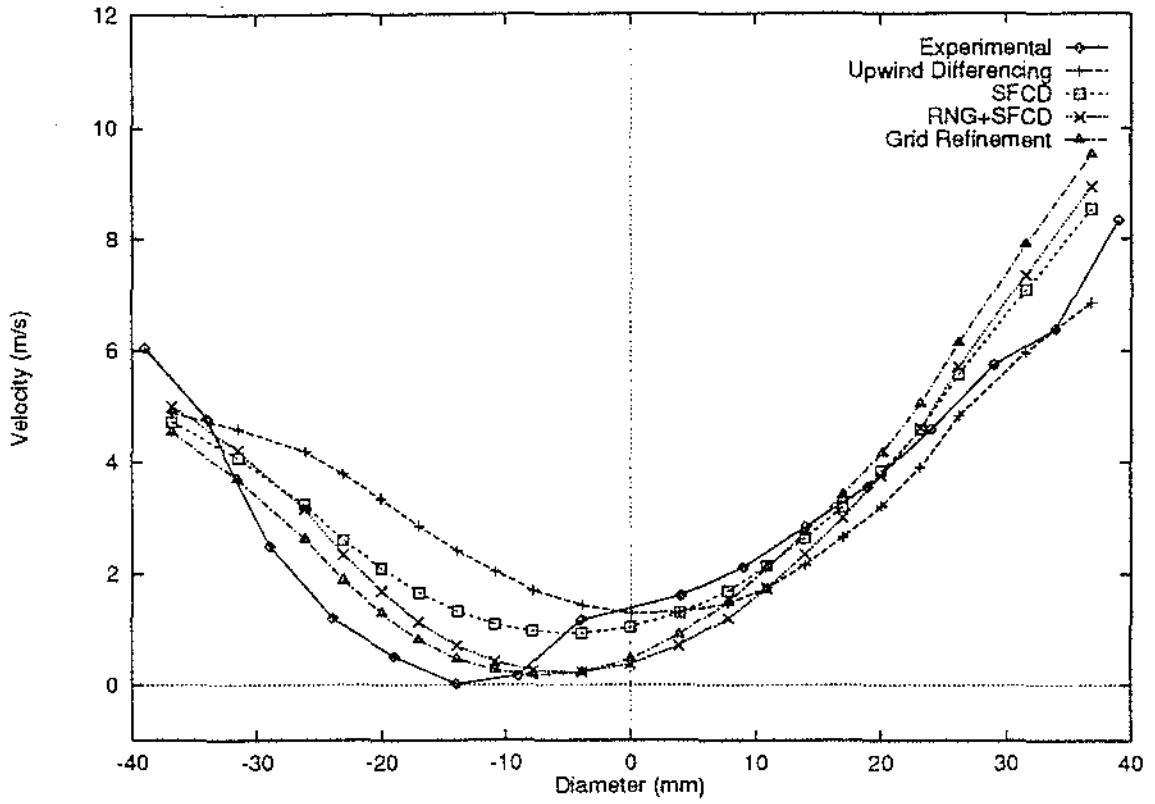
Figure 5a - Axial Velocity Profiles Section A-A: 10 mm Valve Lift
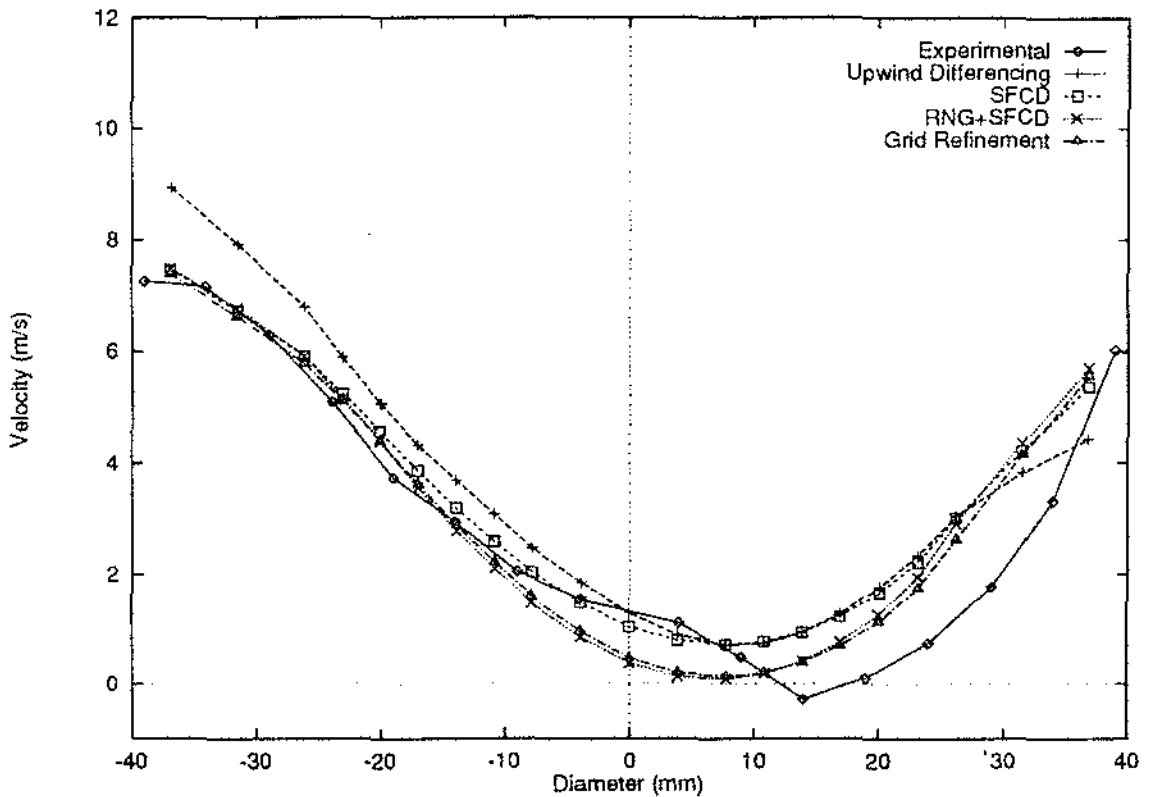
Figure 5b - Axial Velocity profiles section B-B: 10 mm Valve Lift
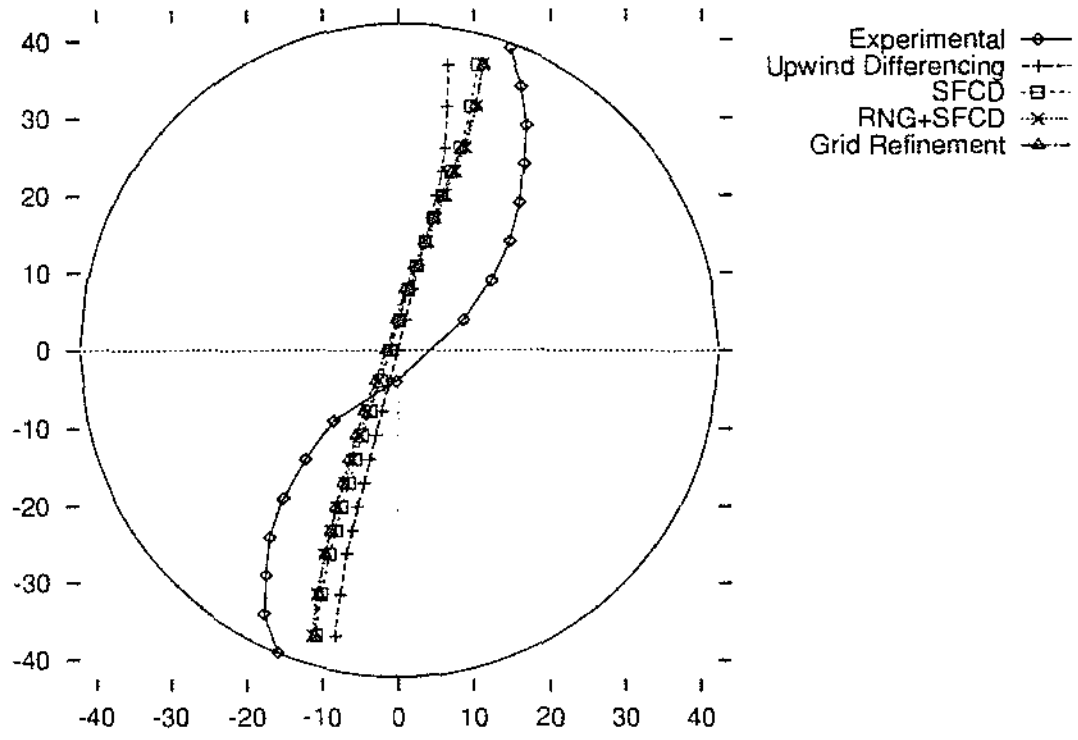
Figure 6a - Swirl Velocity profiles Section A-A: 10 mm Valve Lift
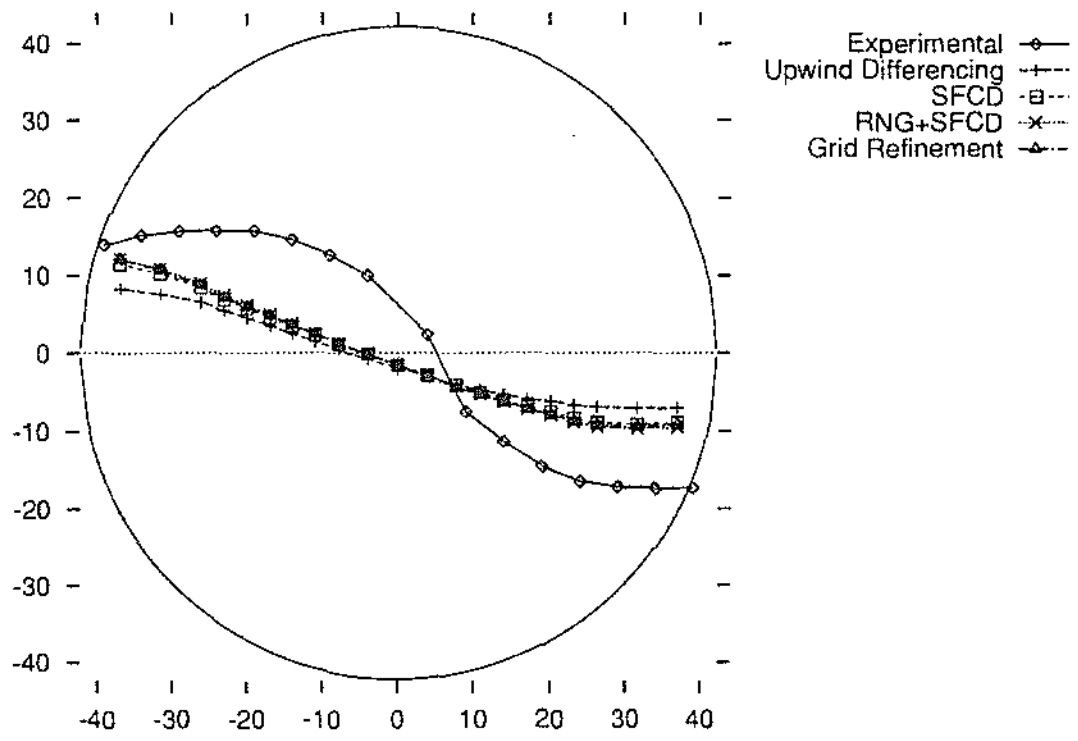
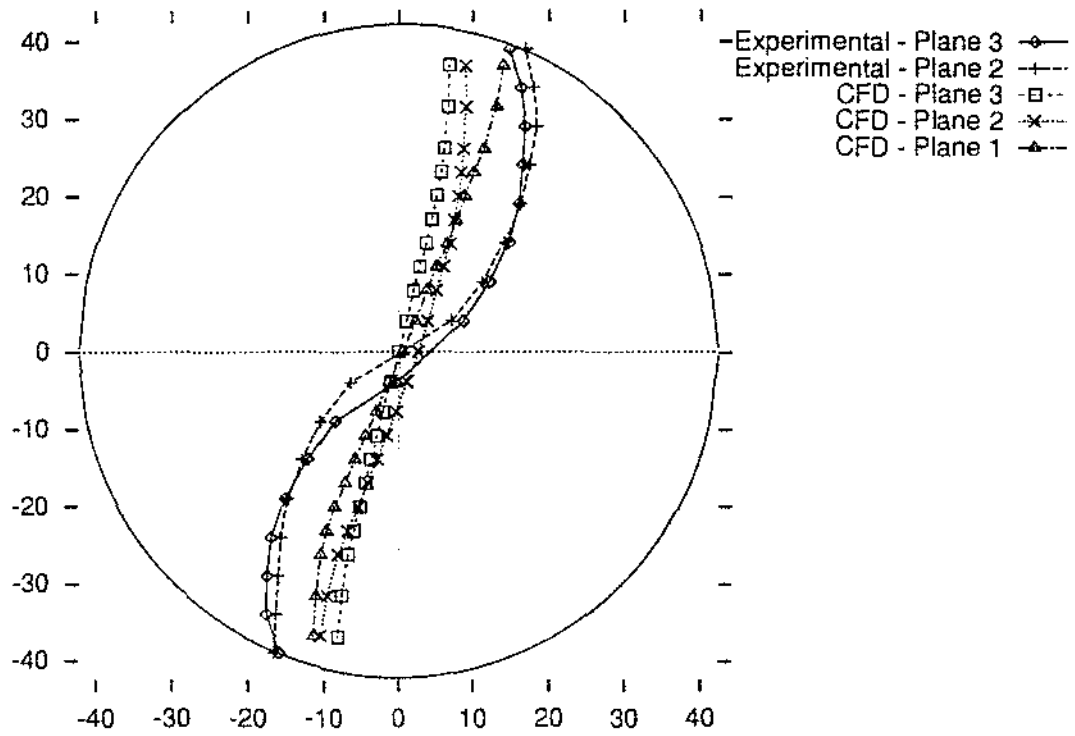**Figure 6b** - Swirl Velocity Profiles Sction B-B: 10 mm Valve Lift

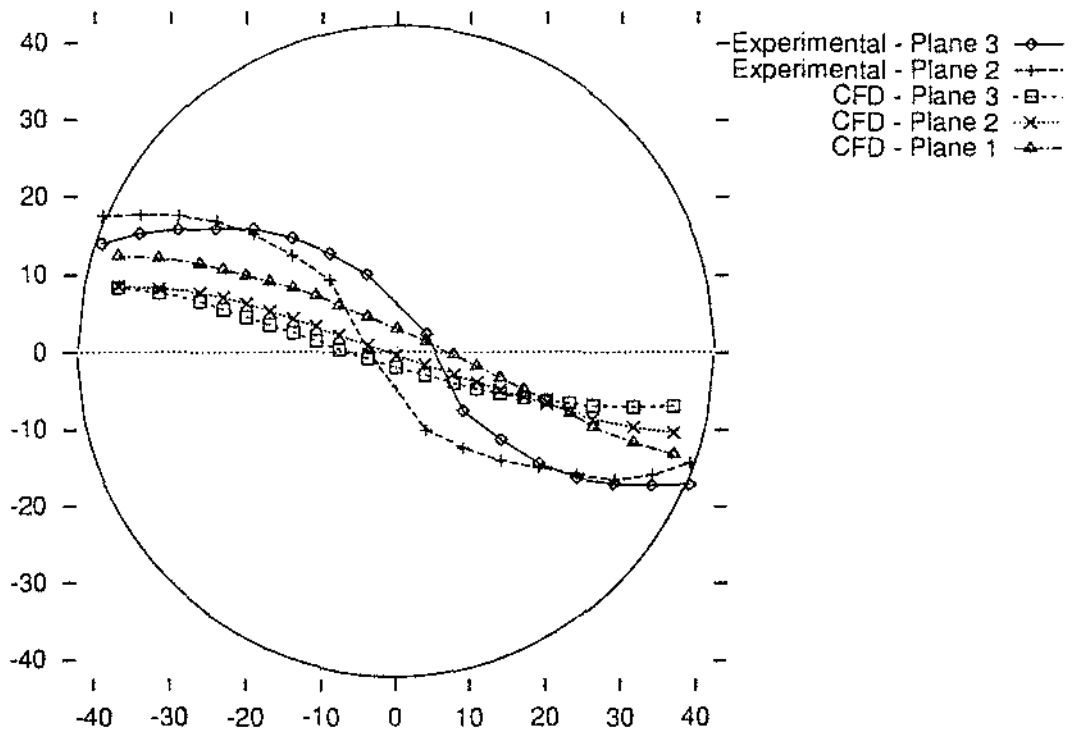**Figure 7a** - Swirl Velocity Profiles Section A-A: 10 mm Valve Lift

Figure 7b - Sxirl Velocity Profiles Section B-B: 10 mm Valve Lift
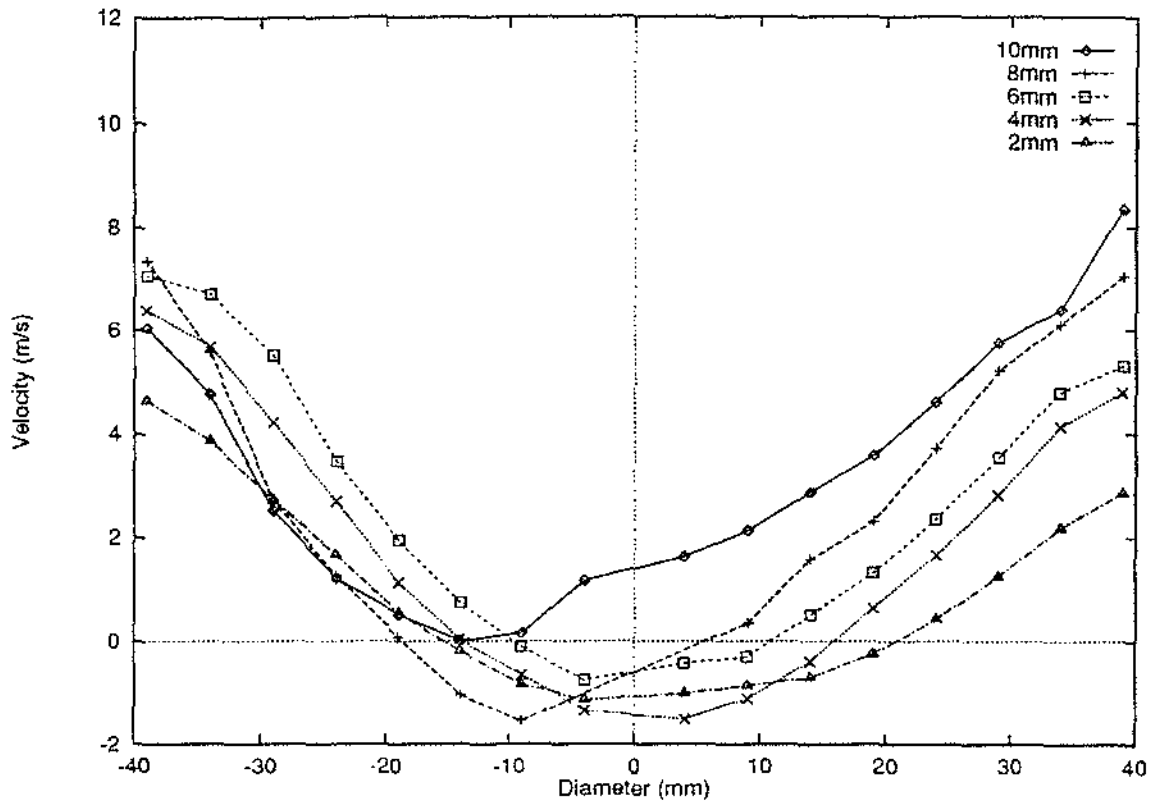
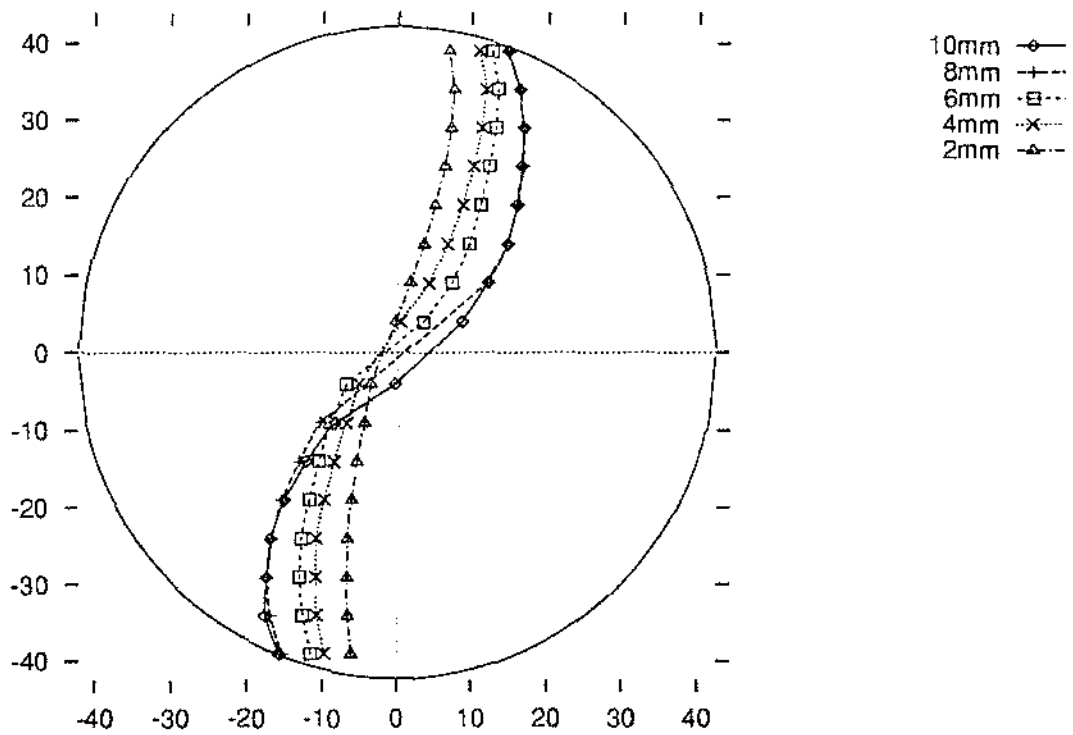**Figure 8a** - Axial Velocity Section A-A: Various Valve Lifts

Figure 8b - Swirl Velocity Profiles Section A-A: Various Valve Lifts